Activation of poly(ethylene terephthalate) surfaces by atmospheric pressure plasma

Tomáš Homola [a,b,c,*], Jindřich Matoušek [d], Beáta Hergelová [b], Martin Kormunda [d], Linda Y.L. Wu [a], Mirko Černák [b,c]

[a] Surface Technology Group, Singapore Institute of Manufacturing Technology, 71 Nanyang Drive, Singapore 638075, Singapore
[b] Department of Experimental Physics, Faculty of Mathematics, Physics and Informatics, Comenius University, Mlynská dolina, 842 48 Bratislava, Slovakia
[c] R&D Center for Low-Cost Plasma and Nanotechnology Surface Modification, Masaryk University, Kotlářská 2, 611 37 Brno, Czech Republic
[d] Department of Physics, J.E. Purkinje University, České mládeže 8, 400 96 Ústí nad Labem, Czech Republic

ABSTRACT

We report a study on effects of atmospheric pressure plasma treatment of poly(ethylene terephthalate) PET surfaces. The atmospheric pressure plasma was generated using Diffuse Coplanar Surface Barrier Discharge (DCSBD) in ambient air. The changes in wettability of PET surfaces were studied by water contact angle measurement. The surface energy was calculated using van Oss–Chaudhury–Good model from contact angles of water, ethylene and diiodomethane. The changes in surface chemistry after the plasma treatment were studied by X-ray photoelectron spectroscopy (XPS). We also observed changes in surface roughness investigated by Atomic force microscopy (AFM). We found that DCSBD plasma treatment for 1 s led to decrease of water contact angle from 78.4° to 40.1°. The surface energy analysis showed that water contact angle decrease is related to increase of polar part of surface energy. XPS measurement confirmed that the plasma treatment led to increase of polar groups on PET surface which explained the changes in surface energy. AFM investigation showed that plasma treatment led to an increase of surface roughness, which could be a benefit for further processing of PET, because higher roughness increases surface area, which can result into higher adhesion between PET and coatings.

© 2012 Elsevier Ltd. All rights reserved.

1. Introduction

PET is widely used as an insulating material in the electrical industry, packaging, protective or decorative coatings for its superior bulk properties, such as transparency, high strength-to-weight ratio, thermal resistance, flexibility and robustness [1]. Nowadays the most interesting is utilization of PET for optoelectronic applications including rollable displays, conformable photo-voltaic and energy-efficient flexible solid-state lightning [2,3]. The growing interest is in flexible panel displays and flexible organic solar cells consisting of PET as a substrate and their production in roll-to-roll line [4,5]. Unfortunately, the PET exhibits low surface energy which can lead to low adhesion between PET and conductive coating, e.g. ITO [2,6] or PEDOT:PSS [7]. Therefore the surface energy of PET must be increased and this process is usually called activation. Many studies showed that a cold plasma treatment is an effective tool for increasing the surface energy of PET. Cold plasma consists of high energy electrons, low energy gas particles, low energy ions, excited particles and long-lived metastable particles which can be important for the treatment itself; however their contribution was not explained sufficiently. Plasma also consists of photons in UV and visible region, but the efficiency of UV irradiation on PET wettability is low [8,9].

Most of the reported plasma sources are inconvenient for roll-to-roll technology because they operate at low pressure [10–14]. Furthermore many atmospheric pressure plasma sources used for surface treatment of PET are driven in noble gases [15–17] which are expensive and their usage can significantly increase the cost of final products. Therefore the plasma generated at low cost conditions, i.e. driven in ambient air at atmospheric pressure, should be used for example in roll-to-roll line.

In this work we report the study on treatment of PET surfaces by Diffuse Coplanar Surface Barrier Discharge (DCSBD) which generates diffuse plasma of high power density in ambient air at atmospheric pressure. Because of the specific arrangement of electrodes

in coplanar configuration, the DCSBD can be easily introduced also to roll-to-roll line [18]. The PET surfaces treated by DCSBD plasma were investigated by water contact angle measurement to determine the surface energy and wettability. XPS was used to investigate the changes in surface chemistry after the plasma treatment and AFM to observe the changes in surface roughness.

2. Experimental

2.1. Materials and plasma treatments

In this study a 50 μm thick biaxially oriented PET surfaces of crystallinity about 30–40% (ES301250, Goodfellow, UK) were treated by atmospheric pressure plasma. Prior to plasma treatment the PET foil was cut into pieces of dimensions about 5 cm × 5 cm. The atmospheric pressure ambient air plasma was generated by DCSBD plasma source [19]. The principle of DCSBD plasma is based on a coplanar DBD where comb-shape electrodes are embedded in a dielectric. The diffuse plasma is generated in thin 0.3 mm thick flat layer on alumina ceramic which designates the DCSBD to be used especially for treatment of flat surfaces [20]. The DCSBD electrode system was powered by AC HV source of frequency approx. 14 kHz and voltage approx. 20 kV peak-to-peak and the total power in plasma during the experiments was 400 W. The power was monitored via oscilloscope measurements using method described in [21]. The area of generated plasma of DCSBD is 170 cm^2, thus the surface energy density and volume energy density at power of 400 W are approximately 2 W cm^{-2} and 80 W cm^{-3}, respectively. The DCSBD plasma is described in detail [18,22–24]. The plasma treatment was performed in dynamic treatment mode described in [22] and the distance between the treated PET surface and DCSBD ceramic was 0.3 mm.

2.2. Surface analyses

The DSA30 (Krüss GmbH, Germany) was used to measure the profiles of sessile droplets on PET surfaces 5 s after their deposition. The DSA 1.92 software was used to determine the 2 μl sessile droplets contact angles of distilled water, ethylene and diiodomethane. In total 20 measurements per each liquid were used to calculate the free surface energy of PET using van Oss–Chaudhury–Good acid–base approach [25]. In this approach, the total surface energy γ represents the sum of two distinct components: the polar γ^{AB} (acid–base) and dispersive γ^{LW} (Lifshitz–van der Waals). The polar part is given by doubled mean of geometrical value of acid (γ$^+$) and base (γ$^-$) interactions.

The durability of wettability after the plasma treatment was investigated for PET samples treated in plasma for 1 s and 10 s. After the plasma treatment the samples were stored in dark place exposed to ambient air at temperature 24 °C. The surface energy was calculated for contact angles taken 3 h, 6 h, 12 h, 24 h, 48 h, 72 h, 144 h and 288 h after the plasma treatment.

XPS measurements were performed with the hemispherical analyser Phoibos 100 (Specs GmbH, Germany) at take-off angle 90° and the spectra were referenced to the peak of aliphatic C–C bonds at 285.0 eV. The XR-50 (Specs GmbH, Germany) non-monochromatic X-ray source with a spectral line Al Kα (photon energy 1486.6 eV) was used to induce the electron emission. The elemental composition was calculated from survey spectra. Relative sensitivity factor used for O1s peak was 2.93 (and RSF = 1.00 in case of C1s). The electron flood gun was not used for charge compensation. C1s and O1s high resolution spectra were recorded to obtain the information on the bonding of the C and O species. The program CasaXPS was used for the computer processing of the spectra. The Shirley background shape was used and the components used for the peak deconvolutions were

mixed Gauss–Lorentzian lines (70% Gaussian and 30% Lorentzian). The transportation time of sample after the plasma treatment to XPS load-lock chamber was approx. 5 min.

The Veeco Nanoscope IIIa (Veeco Instruments Inc. US) was used to investigate the average surface roughness Ra and RMS surface roughness from 5 μm × 5 μm scans before and after the plasma treatment.

3. Results and discussion

3.1. Surface energy

The DCSBD plasma treatment of PET surface resulted in decrease of water contact angle. In Fig. 1 is shown the dependence of water contact angle on plasma treatment time. The water contact angle of untreated PET surface was 78.4° which is in good agreement with [26]. The plasma treatment for 1 s, 3 s, 5 s and 10 s led to decrease of water contact angle to 40.1°, 38.6°, 36.3° and 36.2°, respectively. Fig. 2 shows total surface energy of PET with respect to plasma treatment time. The total surface energy γ calculated for untreated PET surface was 50.6 mJ m^{-2} and after plasma treatment for 1 s, 3 s, 5 s and 10 s increased to 70.6 mJ m^{-2}, 72.4 mJ m^{-2}, 73.7 mJ m^{-2} and 73.8 mJ m^{-2}, respectively. Since the water contact angle and surface energy is related to wettability, from the Figs. 1 and 2 is apparent that the highest change in wettability, i.e. change of water contact angle and surface energy, was achieved after plasma treatment for 1 s. Prolonging the plasma treatment time had only minimal effect on water contact angle or surface energy. Since water is liquid of polar character the decrease of water contact angle is related only to polar part of the surface energy γ^{AB}. Fig. 2 shows also the components of total surface energy γ, the polar γ^{AB} and dispersive γ^{LW} components. It is apparent that the polar component of surface energy γ^{AB} contributes more to total surface energy than dispersive component γ^{LW}. Therefore it is clear that the plasma treatment predominantly led to increase of polar part of surface energy. Since the standard deviations of the surface energy values were approximately 1 mJ m^{-2} the error bars in Fig. 2 are not shown.

The presented results on water contact angle and surface energy of PET after the plasma treatment differ from those presented by
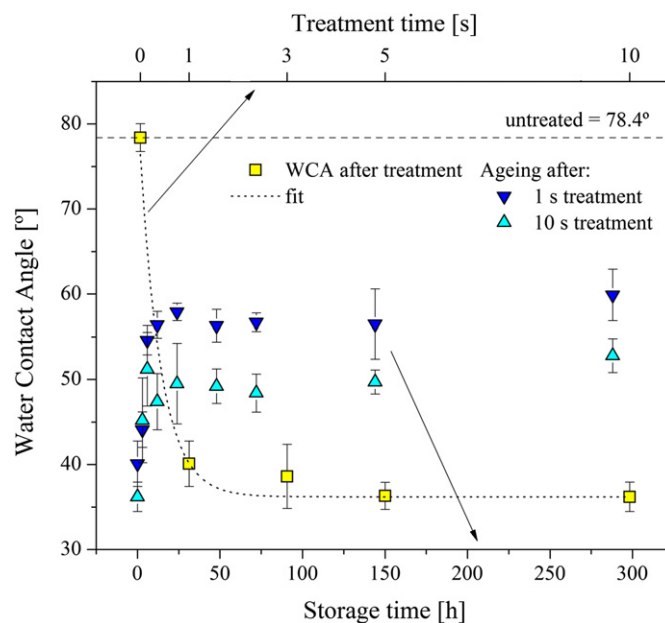

Fig. 1. Contact angle of PET surfaces as a function of plasma treatment time and storage time.
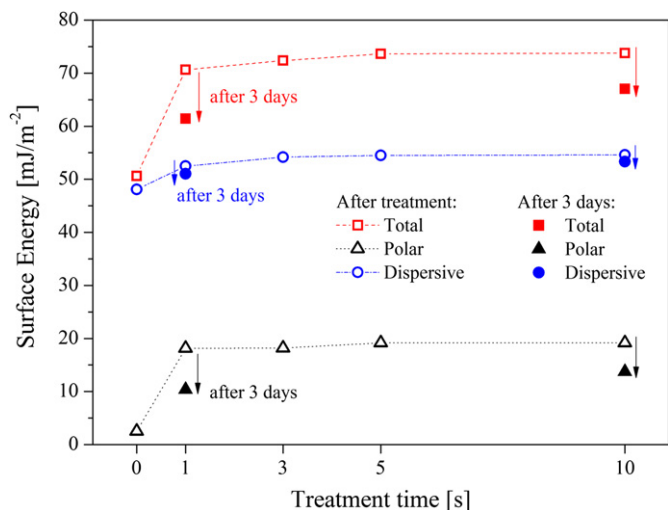
Fig. 2. Surface energy of PET surfaces as a function of plasma treatment time.

Fig. 3. Surface energy of PET surfaces as a function of storage time.

authors using ambient air plasma generated by different DBD's. For example in [26,27] an atmospheric planar DBD air plasma source was used to modify PET surfaces. Similarly to our observations, it was found that plasma treatment leads to decrease of water contact angle and increase of surface energy of PET. However, the comparison of energetic efficiency shows that effectiveness of DCSBD plasma is significantly higher. In order to achieve a decrease of water contact angle from 78° to approximately 40° after plasma treatment for 1 s, a power density in planar DBD was 30 W cm^{-2} whereas DCSBD operated with power density 2 W cm^{-2} and yielded similar values of water contact angles on PET after the plasma treatment compared to [26,27]. The explanation of such high difference in efficiency consists in advantageous technique of DCSBD plasma generation. Whereas the plasma in planar DBD is generated in volume between electrodes of inter-electrode gap 2 mm, the plasma in DCSBD is generated in thin 0.3 mm layer, therefore the energy losses are significantly lower. Furthermore since the DCSBD plasma is generated on the dielectric surface and is not limited by the width of inter-electrode gap, the thickness of the sample treated by DCSBD is unlimited. Therefore is apparent that treatment of the PET surfaces is energetically much efficient by plasma generated using DBD in coplanar configuration rather than in volume configuration.

The surface changes observed after the plasma treatment were not stable when samples were stored in ambient atmosphere. In Fig. 1 is shown the development of water contact angle with respect to storage time for two different samples treated by plasma for 1 s and 10 s. The exposure of the PET surface to ambient air after the plasma treatment led to increase of water contact angle. The water contact angle increase was relatively fast and in first 6 h the water contact angle for samples treated in plasma for 1 s and 10 s increased from 40 1° to 54.6° and from 36.2° to 51.2°, respectively. Nevertheless the rate of hydrophobic recovery observed in 6 h after the plasma treatment was high, 12 days of ambient air exposure led only to small increase of water contact angle which is shown in Fig. 1. Further ageing for 90 days of the plasma treated PET surface for 10 s led to further increase of contact angle to 55.6° (not shown in Fig. 1). Since the water contact angle achieved immediately after the plasma treatment for samples treated in plasma for 1 s and 10 s was similar, only benefit of longer plasma treatment was higher stability of the surface modification and lower rate of surface hydrophobic recovery. Since the water contact angle of untreated PET was 78.4°, these results show that the DCSBD plasma treatment led to permanent changes on the surface.
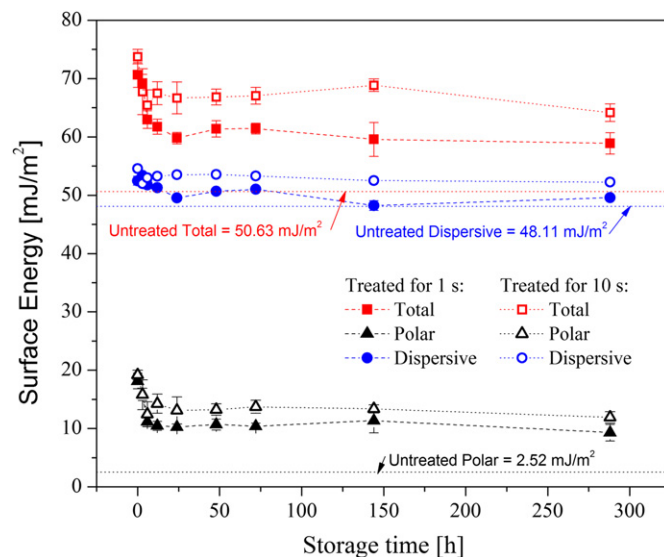
The development of surface energy during the exposure of plasma treated PET surfaces to ambient air was also investigated. In Fig. 2 is shown the decrease of the surface energy when treated samples were exposed to ambient air for 3 days. The Fig. 3 shows the overall decrease of the surface energy for samples treated by plasma for 1 s and 10 s. As was expected from the water contact angle analysis the highest decrease due to ageing was observed for polar component of the surface energy γ^{AB}. Comparison of plasma treated samples for 1 s and 10 s showed that hydrophobic recovery of both components of surface energy γ^{AB} and γ^{LW} is slower for sample treated in plasma for 10 s. The surface energy analysis also confirms that the major benefit of longer treatment time is higher stability of the surface achieved by plasma treatment. The observed phenomenon of PET surface wettability degradation achieved after the plasma treatment is in agreement with the findings reported elsewhere [27–29].

3.2. Surface chemistry

The XPS was used to investigate the chemical state of PET surfaces before and after the plasma treatment. The comparison of
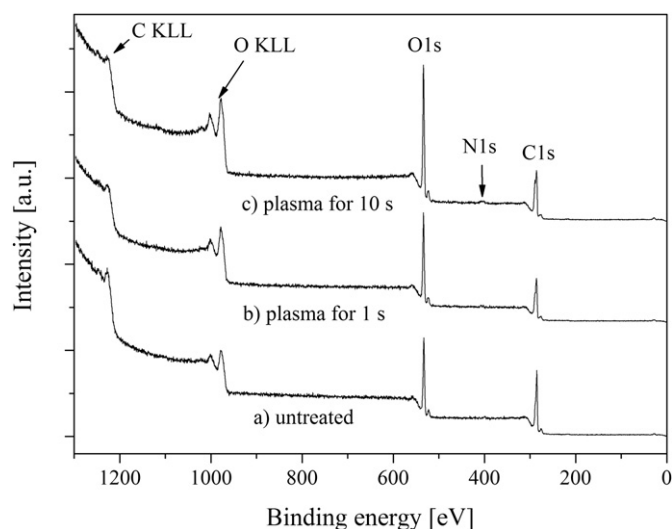

Fig. 4. XPS survey spectra of a) untreated PET surface and PET surface treated by plasma for b) 1 s and c) for 10 s.

Table 1
Elemental composition of PET surfaces treated by plasma for various times.

Sample designation	C1s [%]	N1s [%]	O1s [%]	O/C
Theoretical	71.4	0	28.6	0.40
Untreated	71	1	28	0.39
1 s plasma	62	2	36	0.58
3 s plasma	58	2	39	0.67
5 s plasma	57	3	40	0.70
10 s plasma	60	1	39	0.65
1 s plasma after 3 days	63	2	34	0.54
1 s plasma after 10 days	65	2	32	0.49
10 s plasma after 3 days	63	1	36	0.57

Table 2
Concentrations of molecular functionalities of PET surfaces treated by plasma for various times.

	Concentration [%]				
	C1s			O1s	
	C–C, C–H	C–O	O–C=O	C–O	C=O
	285 eV	286.5 eV	288.9 eV	533.5 eV	531.9 eV
Untreated	59	24	18	56	44
1 s plasma	48	27	25	70	30
3 s plasma	46	26	28	73	27
5 s plasma	42	28	31	76	24
10 s plasma	43	24	33	80	20
1 s plasma after 3 days	48	29	23	62	38
1 s plasma after 10 days	50	27	23	64	36
10 s plasma after 3 days	49	27	25	64	36

survey spectra for untreated PET and PET treated by plasma for 1 s and for 10 s are shown in Fig. 4. The results in Fig. 4 show that PET surfaces contain carbon, oxygen and small amount of nitrogen and differ only in O/C ratio. The Table 1 summarizes the results of concentrations of carbon, oxygen and nitrogen obtained from survey spectra of untreated PET surface and PET surfaces treated by plasma for 1 s, 3 s, 5 s and 10 s. It can be seen that concentration of elements found on untreated PET correlates with the theoretical concentrations of PET. The results in Table 1 show that plasma treatment for 1 s led to decrease of carbon concentration on PET surface from 71 at.% to 62 at.%. Prolonging the plasma treatment time had no additional significant effect on carbon concentration and it remained at 60 at.% after plasma treatment for 10 s. The plasma treatment for 1 s led to increase of oxygen concentration on PET surface from 28 at.% to 36 at.%. Similarly as development of carbon concentration for longer treatment times was negligible, prolonging the plasma treatment time had no significant influence on the oxygen concentration which remained at 39 at.% after the plasma treatment for 10 s. The Table 1 also shows that small amount of nitrogen was found on the PET before and after plasma treatment. However, the concentrations were found small and within the XPS accuracy therefore no conclusion can be made. The Table 1 contains also the O/C ratio which corresponds well with the wettability of the PET surface. The comparison of the data between Table 1, Figs. 1 and 2 shows that increase of O/C ratio on PET surfaces after the plasma treatment was accompanied by decrease of water contact angle and increase of surface energy. To explain the correlation between wettability and O/C ration, the C1s and O1s high-resolution peaks were studied.

The C1s peak was deconvoluted into three components as is shown in Fig. 5. The components at binding energies (C1) 285 eV, (C2) 286.5 eV and (C3) 288.9 eV were attributed to (C1) C–C or C–H, (C2) C–O and (C3) O–C=O or O–C–OH bonds, respectively [30–32]. After the plasma treatment for 1 s the component (C1) decreased from 59% to 48%. The concentration of component (C2) and (C3) increased after plasma treatment for 1 s from 24% to 28% and from 18% to 25%, respectively. This increase is probably related to formation of oxygen-containing groups on PET surfaces. The analysis of C1s peak of PET surfaces treated by plasma for various times is shown in Table 2. The results in Table 2 show that prolonging the plasma treatment time led to decrease of component (C1) and it remained at 43% after plasma treatment for 10 s. The concentration of (C2) varied with respect to plasma treatment time, however the differences were small and no regular trend was observed. The reason for this occurrence is probably a result of C1s deconvolution uncertainty. Whereas some authors deconvoluted C1s peak of PET into four different components [16], other authors used three components [27,30]. We used deconvolution into three components because the XPS had no monochromator and the close components would be hardly distinguished, and moreover, the deconvolution of C1s into four components showed multiple mathematically correct results. This approach has an obvious limitation when C1s is interpreted, but on the other hand the deconvolution had only one mathematically correct result.
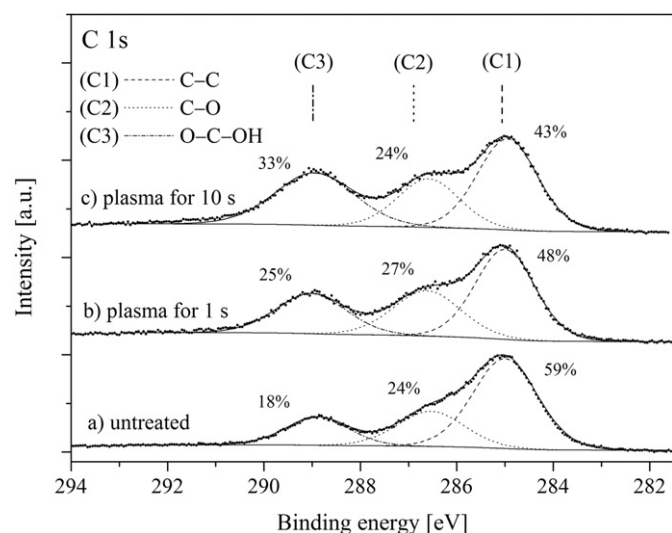

Fig. 5. XPS C1s high resolution peak of a) untreated PET surface and PET surface treated by plasma for b) 1 s and c) for 10 s.
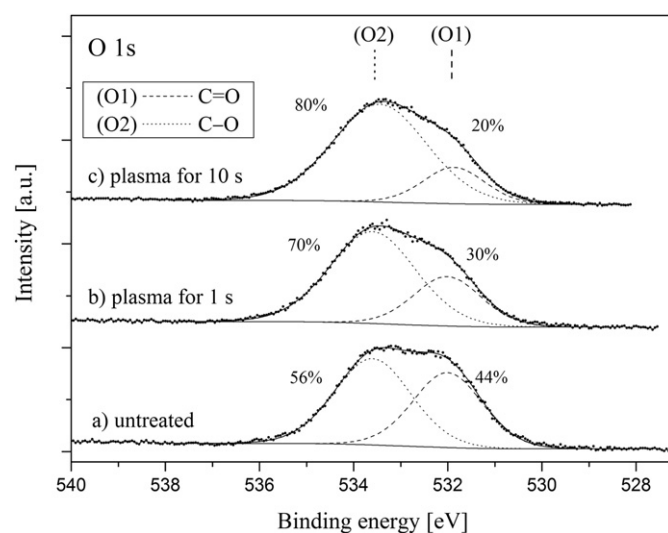

Fig. 6. XPS O1s high resolution peak of a) untreated PET surface and PET surface treated by plasma for b) 1 s and c) 10 s.

Table 3
The RMS and Ra roughness values of PET surface modified by plasma for various times.

Sample designation	RMS roughness [nm]	Ra roughness [nm]
Untreated	1. 87 ± 1.08	1.25 ± 0.84
1 s plasma	6.92 ± 1.92	5.35 ± 1.61
3 s plasma	9.18 ± 2.63	7.19 ± 3.70
5 s plasma	8.32 ± 1.72	5.88 ± 0.81
10 s plasma	10.40 ± 0.55	6.90 ± 0.50

Independently of the four or three component approach, all the authors usually assign the C1s components with non zero chemical shift to oxygen containing groups (zero chemical shift is related to C—C bonds). In our approach of C1s interpretation we found the component (C2) was not affected by the plasma treatment significantly. The peaks related to C—N or O—C—N groups could also contribute to (C2) or (C3), however, as the concentration of N was small, and this contribution was neglected. The concentration of component (C3) increased from 18% to 33% after the plasma treatment for 10 s. As is shown in Table 2 the development of concentration of (C3) is clearly increasing with respect to plasma treatment time. The higher concentration of (C3) component usually attributed to O—C=O groups is related to decrease of water contact angle shown in Fig. 1. The O—C=O group has a polar character and thus a higher concentration of these polar groups can result in higher polar surface energy which was found after the plasma treatment as Fig. 2 shows. Also the development of water contact angle and (C3) component with respect to plasma treatment time seems to be similar. However, (C3) component can also have an origin in presence of O—C—OH group which is discussed below.

The O1s peak was deconvoluted into two components as is shown in Fig. 6. The components at binding energies (O1) 531.9 eV and (O2) 533.5 eV were attributed to (O1) C=O and (O2) C—O bonds [30,33,34], respectively. After the plasma treatment for 1 s the component (O1) decreased from 44% to 30% whereas concentration of component (O2) increased from 56% to 70%. The analysis of O1s peak of PET surfaces treated in plasma for various times are shown in Table 2. The results in Table 2 show that prolonging the plasma treatment time led to decrease of component (O1) and it remained at 20% after plasma treatment for 10 s. The concentration of component (O2) increased to 80% after plasma treatment for 10 s. This finding seems to be contradictory to the deconvolutions of the C1s peak if only O—C=O groups contribution to (C3) is considered. From this point of view, an increase of (O1) related to C=O would be expected. However, O1s peak showed decrease of (O1) related to C=O and increase of (O2) componetnt related to C—O. This can be explained by a formation of C—OH groups after the plasma treatment created on C atoms which are in neighbour positions to O atoms in PET chain. A formation of C—OH yields O—C—OH which contributes only to (C3) component and (O2) component. Therefore an explanation considering a formation of the hydrophilic OH groups brings C1s and O1s measurements to agreement, because the main contribution to (C3) component of C1s peak is due to O—C—OH groups. The ageing effect investigated by XPS (Table 2) showed decrease (C3) component of C1s peak. The (C3) component was ascribed to O—C—OH hydrophilic groups and decrease of their concentration had effect on water contact angle and surface energy as is shown in Figs. 1 and 3, respectively. The XPS observations are in agreement with the surface hydrophobic recovery discussed in Figs. 2 and 3. The PET surface treated by plasma for 1 s showed the (C3) concentration of 25% and exposure of this surface to ambient air (storage time) for 3 days decreased the (C3) concentration to 23%. The exposure to ambient air for 10 days had no additional effect on (C3) intensity and remained at 23%.

The effect of air exposure on the (C1) component of the PET was also observed. The plasma treatment for 1 s and for 10 s had only minor effect on the (C1) component. During the ageing of PET treated by plasma for 10 s the (C1) component increased from 48% to 50% in case of 10 s plasma treatment, which could be due to carbon contaminants from the ambient atmosphere.

These observations on C1s peak showed that asymptotic decrease of water contact angle (Fig. 1), which remained lower than water contact angle of untreated PET even after 10 days of ageing, can be explained by initial fast decrease of component (C3) which remained constant when air exposure (storage time) was prolonged. The decrease of polar part of surface energy with respect to storage time can be explained mainly by decrease of concentration of polar groups on PET surface as the XPS measurement showed.
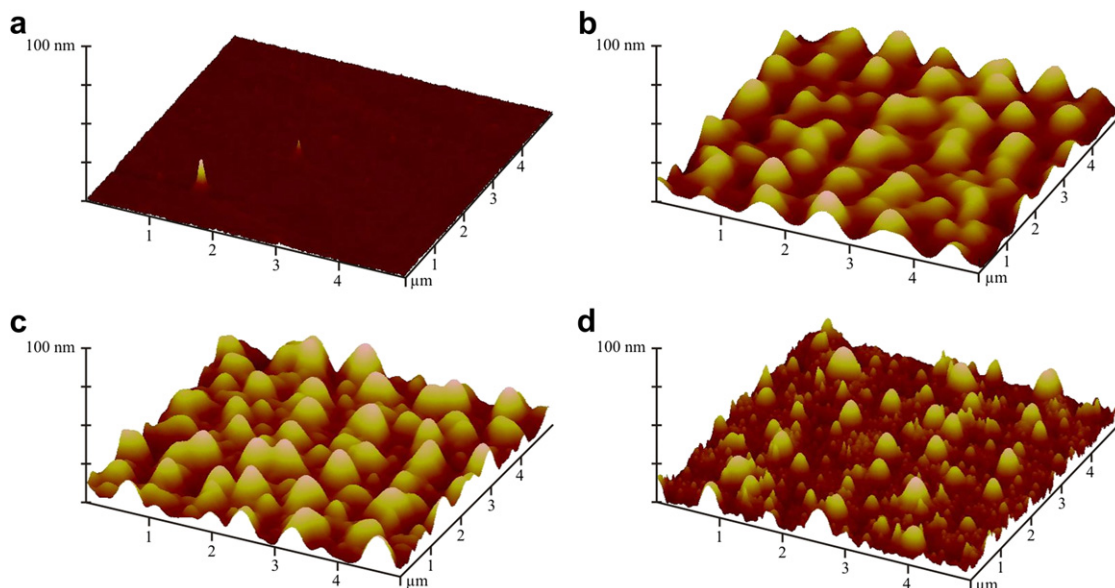

Fig. 7. 3D AFM scans of 5 μm × 5 μm area for a) untreated PET surface and PET surface treated by plasma for b) 1 s, c) 3 s and d) 5 s.

3.3. Surface morphology

The surface morphology of PET surfaces treated by DCSBD plasma was investigated by AFM on randomly selected positions of 5 μm × 5 μm areas. The changes in morphology were quantified by root mean square (RMS) roughness and average roughness Ra. The Table 3 shows the values of RMS and Ra roughness for untreated PET and PET treated by plasma for 1 s, 3 s, 5 s and 10 s. The untreated PET exhibits RMS roughness 1.87 nm and Ra roughness 1.25 nm. The plasma treatment for 1 s led to increase of the RMS roughness and Ra roughness to 6.92 nm and 5.35 nm, respectively. Increase of the plasma treatment time led to higher surface roughness as is shown in Table 3. The 3D AFM scans of untreated PET and plasma treated PET for 1 s, 3 s and 5 s are shown in Fig. 7. In our previous work [22] we found that DCSBD plasma treatment of amorphous PMMA leads to lower surface roughness. The degradation of the surface as is seen in Fig. 7 can be explained by crystalline character of biaxially oriented PET which was about 30–40%. Ref. [35] shows that the plasma treatment of PET with different crystallinity led to etching of predominantly amorphous parts of PET whereas the crystalline regions remained unaffected. Therefore the plasma treatment led to higher surface roughness and since the etching rate of crystalline parts is slower than etching rate of amorphous parts, the roughness can vary with respect to plasma treatment times (see Table 3). The change in surface roughness can lead to change in surface wettability [36]. The increase in roughness increased the area of the surface which can be a benefit for further processing of PET, e.g. applying coating which can results in higher adhesion between PET and coating due to larger active area.

4. Conclusion

The study on effects of DCSBD plasma treatment on surface properties of PET is presented in this paper. The DCSBD plasma treatment for 1 s led to considerable decrease of water contact angle from 78.4° to 40.1°. The comparison of results with other DBD's driven in ambient air showed considerable higher efficiency of DCSBD plasma in order to decrease of water contact angle. This was explained by high efficiency of plasma generated using coplanar arrangement of electrodes in DCSBD. The surface energy analysis via contact angle study of three liquids on PET surfaces showed mainly increase of polar part of surface energy after the plasma treatment. XPS measurements showed that plasma treatment resulted in increased oxygen concentration on PET surfaces. A detailed analysis of high resolution C1s and O1s peaks showed an increase of oxygen-based polar groups, mainly C–OH present in O–C–OH chains. The increased concentration of polar groups observed by XPS correlated with surface energy measurements. We found that the surface energy achieved by the plasma treatment was not stable. However, permanent changes on surface energy were observed. The partial hydrophobic recovery after plasma treatment was confirmed by XPS measurements which showed a decrease of hydrophilic polar group concentration with respect to ambient air exposure time. The plasma treatment led to increase of surface roughness which was explained by a crystalline character of PET surfaces. The higher surface roughness could be also a benefit of the plasma treatment because higher roughness leads to higher surface area which can increase an adhesion between PET and coating.

References

[1] Choi MC, Kim Y, Ha CS. Progress in Polymer Science 2008;33:581.
[2] Sierros K, Morris N, Kukureka S, Cairns D. Wear 2009;267:625.
[3] MacDonald WA. Journal of Materials Chemistry 2004;14:4.
[4] Crawford GP. Flexible flat panel displays. John Wiley & Sons; 2005.
[5] Logothetidis S. Materials Science and Engineering B 2008;152:96.
[6] Choi KH, Jeong JA, Kang JW, Kim DG, Kim JK, Na SI, et al. Solar Energy Materials and Solar Cells 2009;93:1248.
[7] Dennler G, Sariciftci NS. Proceedings of the IEEE 2005;93:1429.
[8] Praschak D, Bahners T, Schollmeyer E. Applied Physics A 1998;66:69.
[9] Gotoh K, Kikuchi S. Colloid and Polymer Science 2005;283:1356.
[10] Singh N, Qureshi A, Shah N, Rakshit A, Mukherjee S, Tripathi A, et al. Radiation Measurements 2005;40:746.
[11] Lopez-Santos C, Yubero F, Cotrino J, Gonzalez-Elipe AR. ACS Applied Materials & Interfaces 2010;2:980.
[12] Carosio F, Alongi J, Frache A. European Polymer Journal 2011;47:893.
[13] Friedrich J, Loeschcke I, Frommelt H. Polymer Degradation and Stability 1991; 31:97.
[14] Placinta G, Arefi-Khonsari F, Gheorghiu M, Amouroux J, Popa G. Journal of Applied Polymer Science 1997;66:1367.
[15] De Geyter N, Morent R, Leys C, Gengembre L, Payen E, Van Vlierberghe S, et al. Surface and Coatings Technology 2008;202:3000.
[16] Cheng C, Liye Z, Zhan R. Surface and Coatings Technology 2006;200:6659.
[17] Kim EH, Yang CW, Park JW. Current Applied Physics 2010;10:S510.
[18] Černák M, Kováčik D, Ráheľ J, Šťahel P, Zahoranová A, Kubincová J, et al. Plasma Physics and Controled Fusion 2011;53:124031.
[19] Kormunda M, Homola T, Matoušek J, Kováčik D, Černák M, Pavlík J. Polymer Degradation and Stability 2012;97:547.
[20] Černák M, Černáková Ľ, Hudec I, Kováčik D, Zahoranová A. The European Physical Journal Applied Physics 2009;47:22806.
[21] Odrášková M, Ráhel J, Zahoranová A, Tiňo R, Černák M. Plasma Chemistry and Plasma Processing 2008;28:203.
[22] Homola T, Matoušek J, Hergelová B, Kormunda M, Wu YLL, Černák M. Polymer Degradation and Stability 2012;97:886.
[23] Homola T, Matoušek J, Medvecká V, Zahoranová A, Kormunda M, Kováčik D, et al. Applied Surface Science 2012;258:7135.
[24] Šimor M, Ráheľ J, Vojtek P, Černák M, Brablec A. Applied Physics Letters 2002; 81:2716.
[25] van Oss C, Chaudhury MK, Good RJ. Chemical Reviews 1988;88:927.
[26] Fang Z, Yang H, Qui Y. IEEE Transactions on Plasma Science 2010;38:1615.
[27] Fang Z, Wang X, Shao R, Qiu Y, Edmund K. Journal of Electrostatics 2011;69:60.
[28] De Geyter N, Morent R, Leys C. Nuclear Instruments and Methods in Physics Research Section B: Beam Interactions with Materials and Atoms 2008;266: 3086.
[29] Morent R, De Geyter N, Leys C, Gengembre L, Payen E. Surface and Coatings Technology 2007;201:7847.
[30] Inagaki N, Narushim K, Tuchida N, Miyazaki K. Journal of Polymer Science Part B: Polymer Physics 2004;42:3727.
[31] Groning P, Collaud M, Dietler G, Schlapbach L. Journal of Applied Physics 1994;76:887.
[32] Vesel A, Junkar I, Cvelbar U, Kovac J, Mozetic M. Surface and Interface Analysis 2008;40:1444.
[33] Kormunda M, Pavlik J. Polymer Degradation and Stability 2010;95:1783.
[34] Gonzalez E, Barankin MD, Guschl PC, Hicks RF. Langmuir 2008;24:12636.
[35] Jacobs T, De Geyter N, Morent R, Van Vlierberghe S, Dubruel P, Leys C. Surface and Coatings Technology 2011.
[36] Nosonovsky M, Bhushan B. Microsystem Technologies 2005;11:535.